STRUCTURAL
BIOLOGY

Volume 76 (2020)

Supporting information for article:

The crystal structure of AjiA1 reveals a novel structural motion mechanism in the adenylate-forming enzyme family

Fernanda C. R. de Paiva, Karen Chan, Markiyan Samborskyy, Ariel M. Silber, Peter F. Leadlay and Marcio V. B. Dias

Table S1 Data collection and processing

Values for the outer shell are given in parentheses.

Diffraction source	PETRA III, EMBL c/o DESY BEAMLINE P13 (MX1)
Wavelength (Å)	0.976195 Å
Temperature (K)	100
Detector	DECTRIS PILATUS 6M PIXEL
Crystal-detector distance (mm)	438.35
Rotation range per image (°)	0.1
Total rotation range (°)	360
Exposure time per image (s)	0.04
Space group	$P3_121$
a, *b*, *c* (Å)	128.78, 128.78, 101.45
α, β, γ (°)	90, 90, 120
Resolution range (Å)	48.870–2.000 (2.050–2.000)
Total No. of reflections	1320343 (92631)
No. of unique reflections	65461 (4483)
Completeness (%)	99.800 (97.900)
Redundancy	20.200 (20.700)
$\langle I/\sigma(I)\rangle$	24.400 (1.8)
$R_{\text{r.i.m.}}$	0.069 (2.637)
$R_{\text{p.i.m.}}$	0.015
Overall *B* factor from Wilson plot (Å^2)	46.820

Table S2 Structure solution and refinement

Values for the outer shell are given in parentheses.

Resolution range (Å)	33.8160–2.0030 (2.0325–2.0026)
Completeness (%)	99.8
σ cutoff	$F > 1.350\sigma(F)$
No. of reflections, working set	62196 (2564)
No. of reflections, test set	3205 (133)
Final R_{cryst}	0.188 (0.3501)
Final R_{free}	0.224 (0.3892)
No. of non-H atoms	6869
Protein	6713
Ligand	**0**
Solvent	152 **0**
Total	6869
R.m.s. deviations	
Bonds (Å)	0.008
Angles (°)	0.924
Average *B* factors (Å^2)	63.61
Protein	63.74
Ligand	**0.0**
Ramachandran plot	
Most favoured (%)	96
Allowed (%)	4

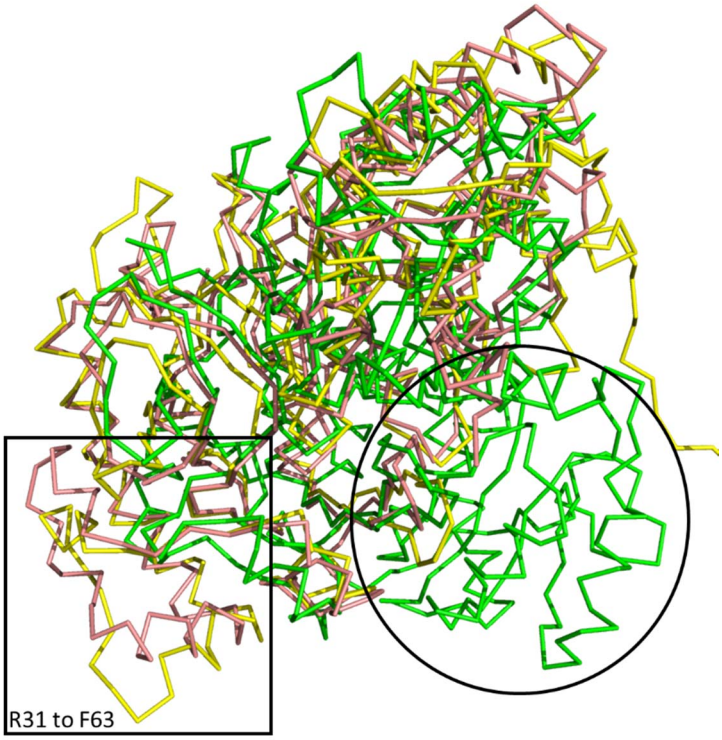

Figure S1 N terminal of Ajia1. AjiA1 (yellow) and PaaK1 (2y27) (salmon) contain a small helical bundle arrangement at the N-terminus (boxed) but lack the typical N-terminal arrangement exhibited by family members (circle). Overlays of AjiA1, PaaK1 and 1mdb, a homolog family member (Protein Data Bank code 1MDB, 2,4-dihydroxybenzoateAMPligase, green) demonstrate the typical α/β-sandwich arrangement at the N terminus (circle).

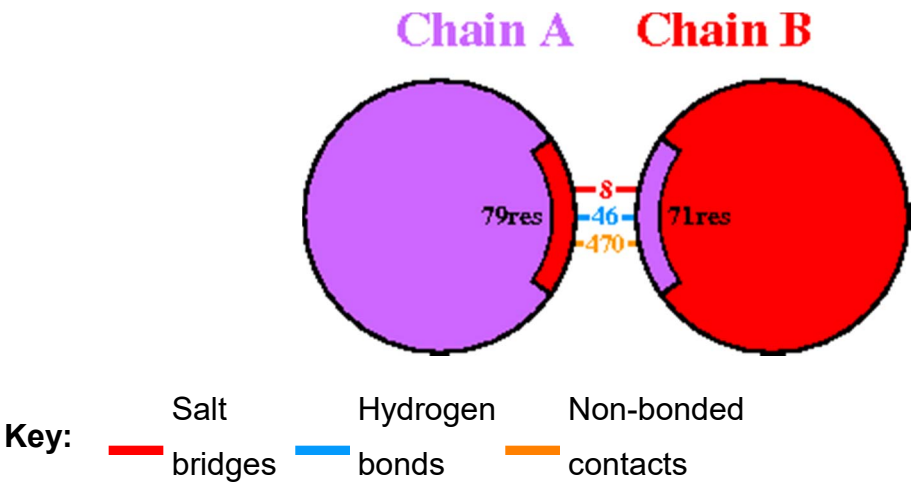

Figure S2 Dimerization interface of AjiA1. The online server PDBsum (Laskowski *et al.*, 2018) (EMBL-EBI) was used to generate a schematic diagram showing the interactions between the two chains of AjiA1. Interacting chains are joined by colored lines, each representing a different type of interaction, orange = non-bonded contacts, blue = hydrogen bonds, and red lines = salt bridges. The area of each circle is proportional to the surface area of the corresponding protein chain. The extent of the interface region on each chain is represented by the black wedge whose size signifies the interface surface area.

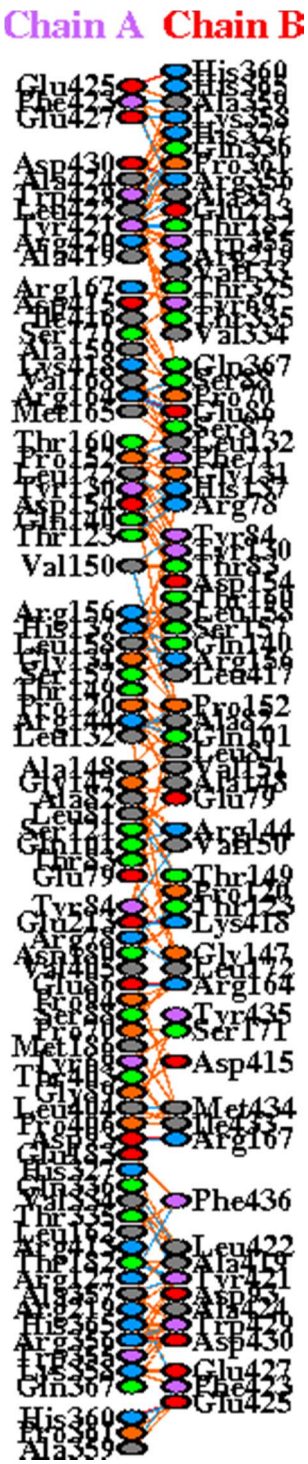

Figure S3 Dimerization interface of AjiA1. The online server PDBsum (Laskowski et al., 2018) (EMBL-EBI) was used to generate a residue interaction net across the interface between the two chains of AjiA1, which are colored by residue type. The number of H-bond lines between any two residues indicates the number of potential hydrogen bonds between them. For nonbonded contacts, which can be plentiful, the width of the striped line is proportional to the number of atomic contacts. Interacting chains are joined by colored lines, each representing a different type of interaction, orange = non-bonded contacts, blue = hydrogen bonds, and red lines = salt bridges. The residue colors are

Positive blue (H, K, R); negative red (D, E); neutral green (S, T, N, Q); aliphatic gray (A, V, L, I, M); aromatic purple (F, Y, W); Proline and Glycine orange.

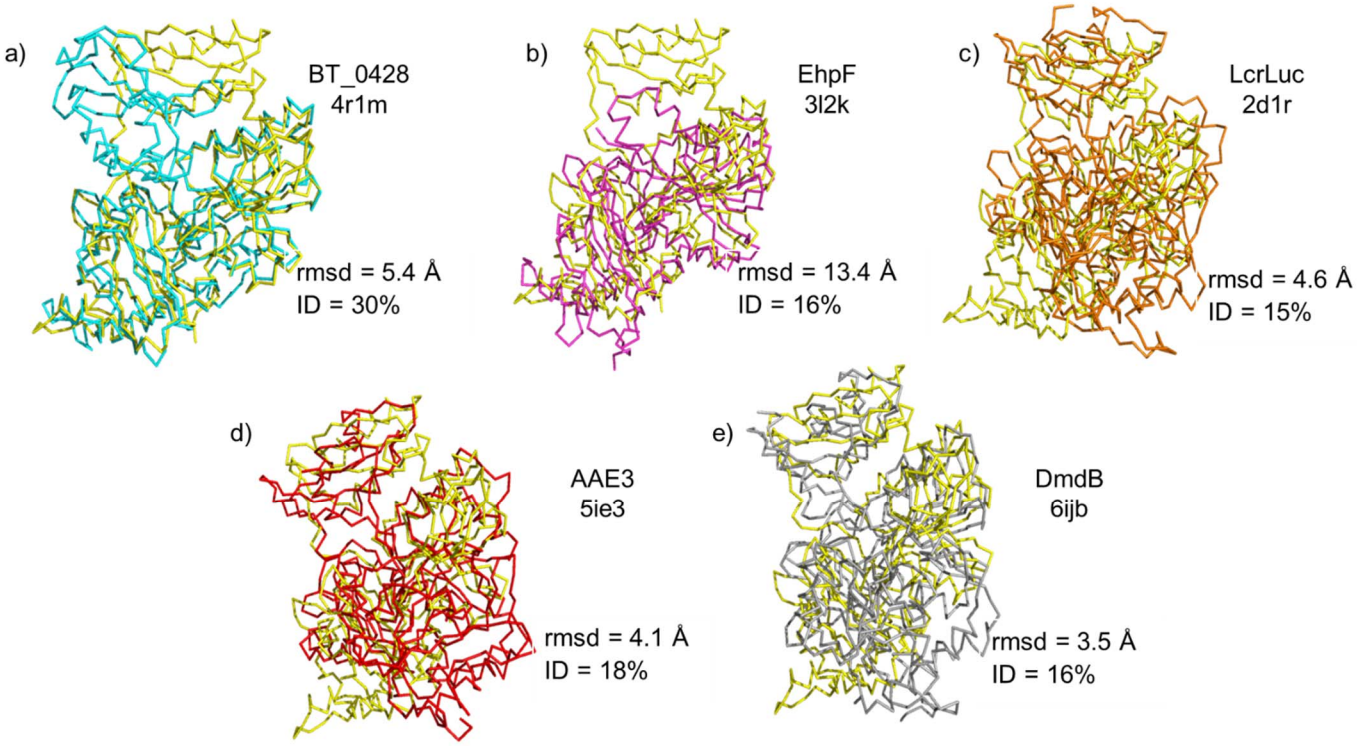

Figure S4 Structural homologs of AjiA1. The Cα chain of AjiA1 was aligned with its structural homologs (a) 4R1M (cyan), (b) 3L2K (purple), (c) 2D1R (orange), (d) 5IE3 (red), and (e) 6IJB (gray). The rmsd value for the superposition with AjiA1 and amino acid identity (%) to AjiA1 is given in each analysis.

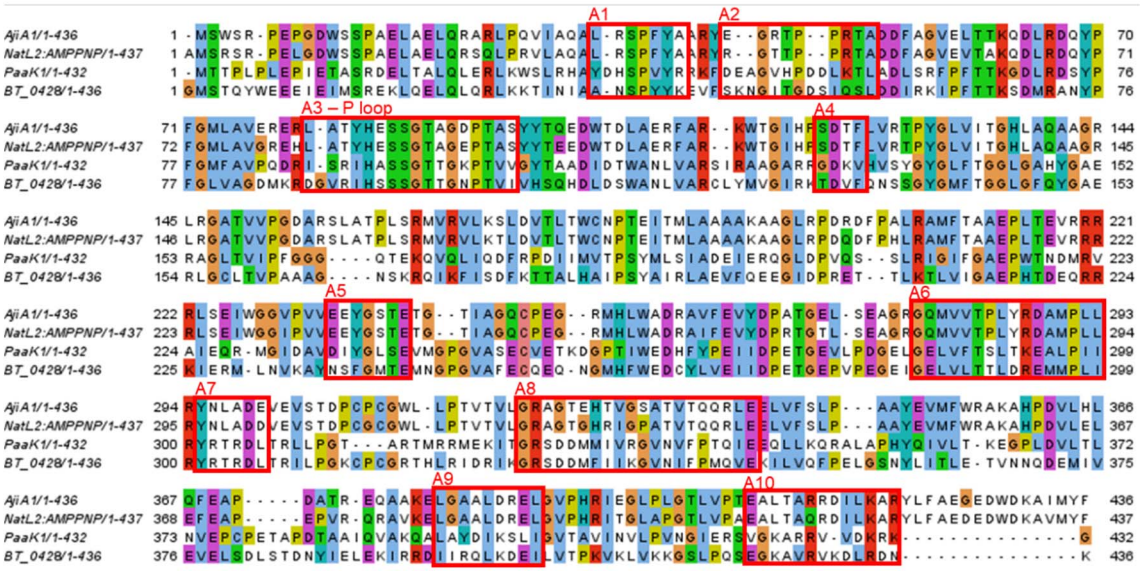

% Identity to AjiA1	
NatL2:AMPPNP	91
PaaK1	30
BT_0428	30

Figure S5 Alignment of AjiA1 and PaaK1 with several DALI homologs. The A1–A10 motifs conserved in the ANL superfamily enzymes are indicated according to the defined adenylation domain of nonribosomal peptide synthetase (Marahiel *et al.*, 1997). Core motifs A1-A10 are shown in red frames. The alignment was generated by ClustalOmega (Sievers *et al.*, 2011) and imported into the Jalview Version: 2.11.0 (Waterhouse *et al.*, 2009). Similar residues are colored accordingly: blue, hydrophobic; green, polar; purple, negative; red, positive; yellow, proline; orange, glycine. The table displays the % identity of AjiA1 to the aligned homologs.

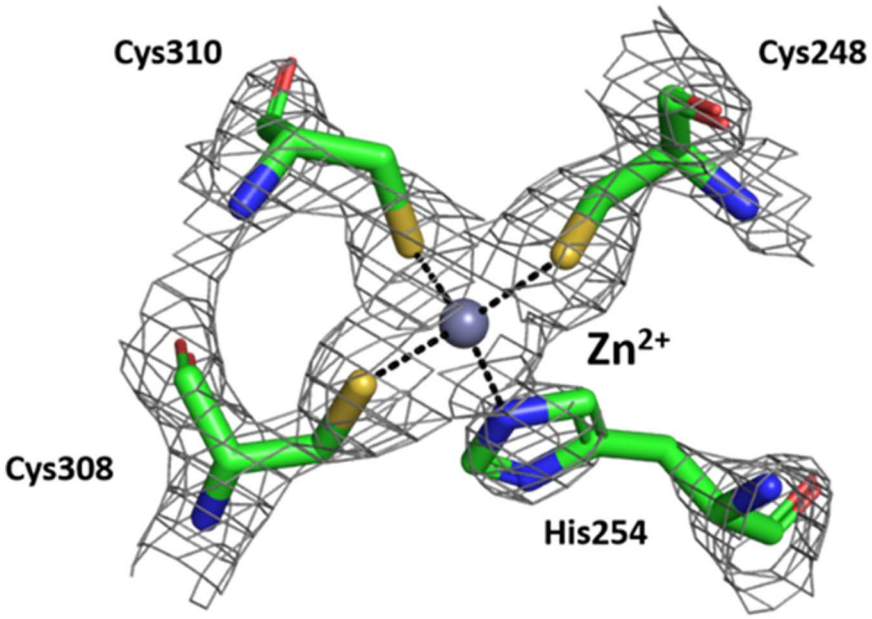

Figure S6 Zinc binding site in the chain A of AjiA1 with an omit map (2Fo–Fc) of Zn^{2+} (contoured to 2.0 σ). This figure shows the coordination interactions.

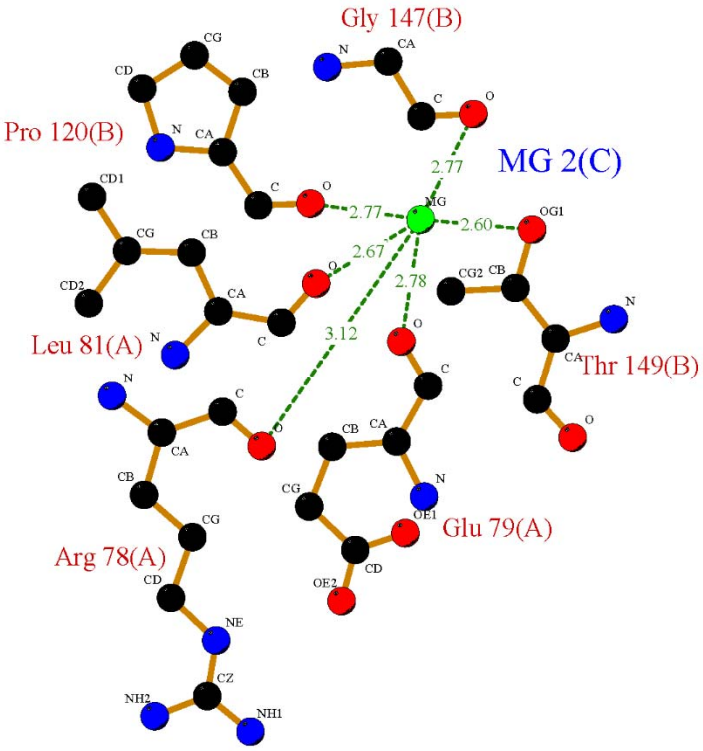

Figure S7 Schematic representation of the Mg^{2+} binding site at chain A of AjiA1. The figure was prepared using LigPlot+ v.2.1 (Laskowski & Swindells, 2011)

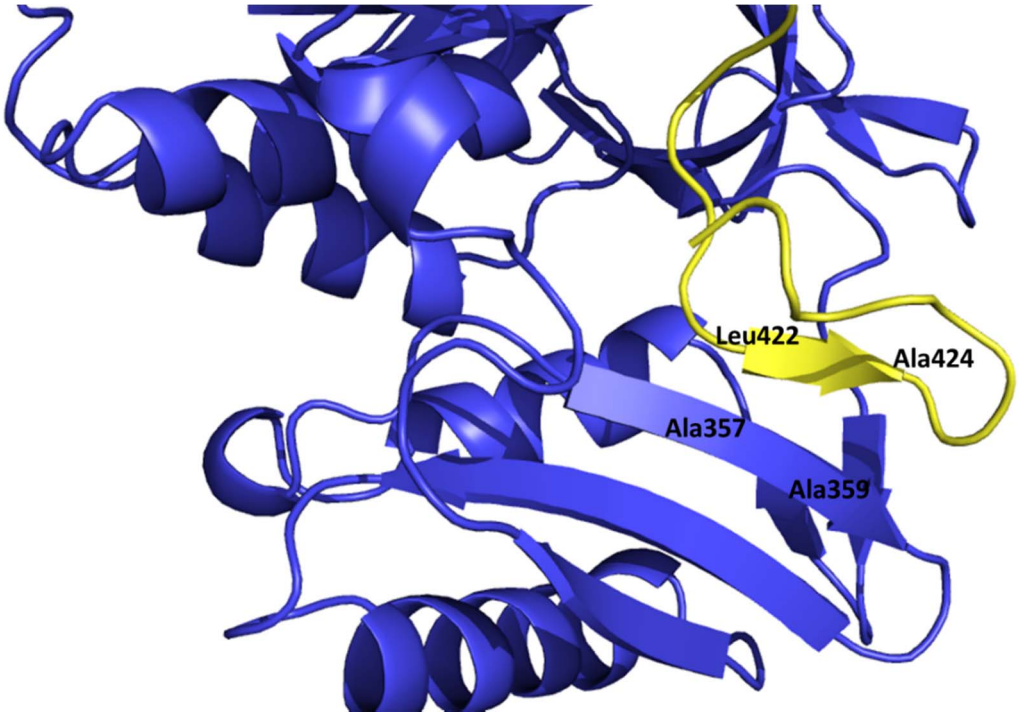

Figure S8 Region of the loop swapping in cartoon view. Amino acids 422L, 423F and 424A appear to form a small beta-strand that could be involved in the formation of a β-sheet with amino acids 357A, 358K and 359A. Chain A is in yellow and chain B is in blue.

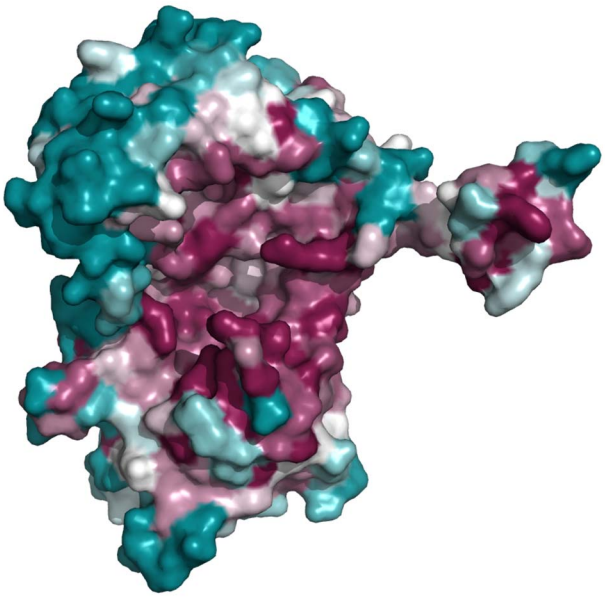

Figure S9 Surface representation of the AjiA1 monomer showing the conservation of residues with other AFE members. The figure was prepared using the ConSurf server (Ashkenazy et al., 2016). Purple and cyan indicate high and low sequence conservation, respectively.

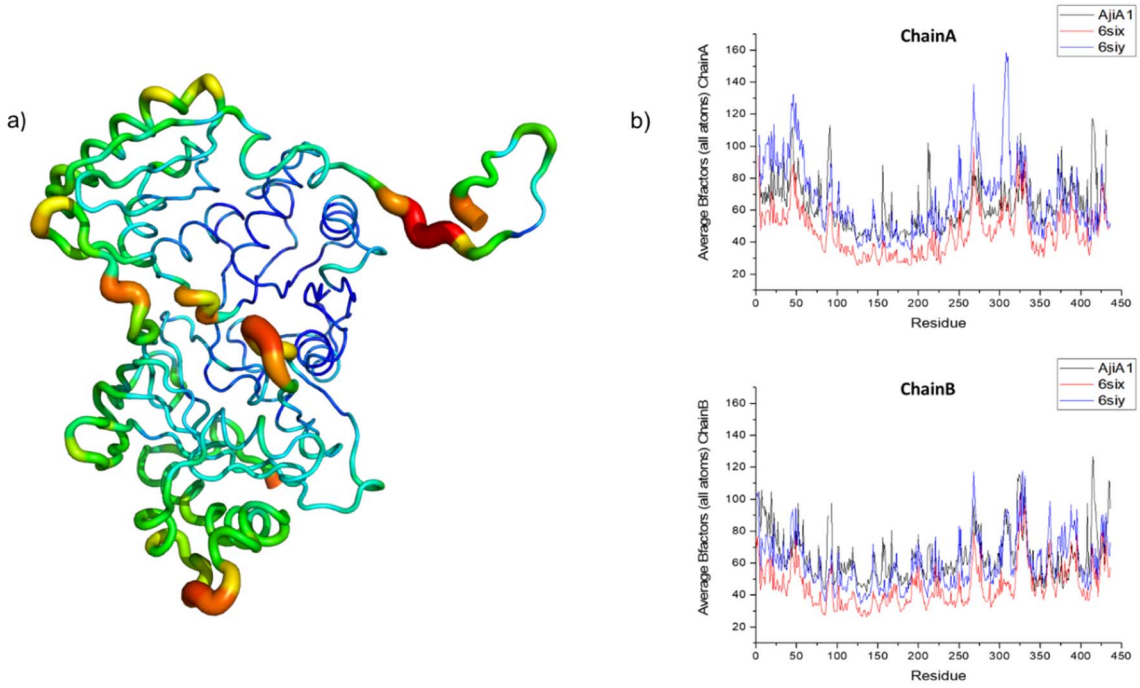

Figure S10 The B-factor putty representation showing the rigid core. (a) The B-factor values are illustrated by color, ranging from low (blue) to high (red), and by shape, a wider tube indicates regions with higher B-factors, whereas a narrower tube indicates regions with lower B-factors. (b) Temperature factor analysis. Graphs of average B-factor versus residue for each chain in AjiA1.